JMEPEG (2011) 20:481–486
DOI: 10.1007/s11665-010-9700-7

1059-9495/$19.00

Thermal Stability and Tensile Properties of Electrodeposited Cu-Bi Alloy

Xianhua Chen and Jianjun Mao

(Submitted November 17, 2009; in revised form April 26, 2010)

By means of pulse electrodeposition technique, a nanocrystalline Cu-0.42at.%Bi alloy with a grain size down to ~10 nm was synthesized. The thermal stability of Cu-Bi electrodeposit was investigated using differential scanning calorimetry (DSC), x-ray diffraction (XRD), transmission electron microscopy (TEM), and hardness measurements. The temperature at which this material tends to become unstable was found to be 160 °C. DSC revealed an exothermal peak between 190 and 300 °C, caused by grain growth. It was observed that segregation of Bi at grain boundary has a considerable effect on the thermal stability of the Cu-Bi alloy. Tensile test showed the sample interestingly possesses a high strength of 760 MPa, while no plastic strain is detected.

Keywords grain growth, nanocrystalline Cu-Bi, segregation, strength, thermal stability

1. Introduction

It is well known that formation of nanocrystalline (nc) structure in metals and alloys leads to remarkable properties (Ref 1). Such materials have attracted much attention since Gleiter (Ref 2) proposed them as being a structurally different state when compared with crystalline or glassy state.

In general, nc materials are thermodynamically unstable, with a strong tendency to transform into a normal polycrystal with coarser grain size. Unfortunately, the materials may lose its improved or novel properties as a result of grain growth. Therefore, their thermal stability is of immense interest for technological applications. In the absence of stresses (applied or residual), the driving force for microstructural degradation is the minimization of total interfacial free energy per unit volume, G_I, which can be written as (Ref 3):

$$G_I = A_I \sum_i \sigma_i f_i \qquad \text{(Eq 1)}$$

where A_I is the total interfacial area per unit volume, σ_i is the interfacial energy per unit area of interface i, and f_i is the corresponding area fraction.

Thermal stability can be enhanced by decreasing G_I, which can be achieved by decreasing A_I and/or by decreasing σ_i. σ_i can be reduced by additions of solute atoms that segregate to the boundaries. The idea that grain boundary segregation may stabilize nc structures has been explored experimentally in the Ni-P, Ni-W, Ni-Mn, Y-Fe, Co-P systems by Kirchheim, Weismmuller, Detor, and Talin et al. (Ref 4-10). For example, Talin et al. (Ref 10) found that nc Ni-0.43at.%Mn deposits exhibit significant thermal stability as compared to pure Ni deposits and retain strength and fine-grained structure up to 500 °C, resulting from the mechanism of Mn segregation at grain boundaries (GBs) for annealing temperature below 600 °C. Similarly, the studies by Farber et al. (Ref 8) revealed a continuous segregation of P in the grain boundaries of nc Ni-3.6at.%P alloy during heat treatment, which could be the explanation to the comparatively high thermal stability of this material.

Cu-Bi alloy has an enormous potential to substitute Cu-Sn alloy that is applied in the pipes of potable water. The Cu-Bi binary system is known to show immiscibility, and the Bi element tends to segregate to GBs of Cu crystallites (Ref 11). The Cu-Bi system represents a classical example for the strong segregation of oversized impurity atoms to the GBs in dilute alloys and has been the subject of detailed investigations in the past several decades of years (Ref 12). Consequently, it is of much interest to explore the effect of Bi addition on thermal stability of nc Cu. In this article, using pulse electrodeposition, we fabricated a nc Cu-0.42at.%Bi sample with average grain size of about 10 nm to systematically study the features of its microstructure and thermal stability.

On the other hand, there is only limited experimental data reported on the tensile behaviors of nc metallic materials with grain size smaller than 15 nm due to the practical difficulty of sample preparation until now (Ref 1). It is necessary to investigate the tensile properties of this electrodeposited Cu-Bi by applying uniaxial tensile measurements.

2. Experimental Procedures

The nc Cu-Bi sample was produced by pulse electrodeposition technique from an electrolyte consisting of $CuSO_4$ and $Bi(ClO_4)_3$. The concentration of Cu^{2+} is 85 g/L, and Bi was

Xianhua Chen, College of Materials Science and Engineering, Chongqing University, Chongqing 400044, People's Republic of China; National Engineering Research Center for Magnesium Alloys, Chongqing University, Chongqing 400044, People's Republic of China and Shenyang National Laboratory for Materials Science, Institute of Metal Research, Chinese Academy of Sciences, 72 Wenhua Road, Shenyang 110016, People's Republic of China and **Jianjun Mao**, College of Materials Science and Engineering, Chongqing University, Chongqing 400044, People's Republic of China. Contact e-mail: xhchen@cqu.edu.cn.

added as $Bi(ClO_4)_3$ at a concentration of 0.5 g/L. Pulsed electrodeposition was carried out galvanostatically using cathodic square wave pulses by turning off the current periodically, with an on-time of 0.02 s and an off-time of 2 s. The peak current density is about 50 A/cm^2 and the pH value is about 1. A highly purified (99.99%) electrolytic copper sheet was used as the soluble anode with gelatin as bath additions in the solutions. The nc Cu-Bi was deposited on a substrate of Ti. The electrolyte was stirred mechanically at a bath temperature of 18 ± 1 °C. Chemical analysis of as-deposited foil removed from the substrate indicated an overall Bi concentration of 0.42 at.%.

The microstructure of the as-deposited sample was characterized using XRD, TEM, and high-resolution TEM (HRTEM). Quantitative XRD measurements of the Cu-Bi samples were carried out in a Rigaku D/MAX 2400 X-ray diffractometer. The (111)/(222) and (200)/(400) peak pairs were used to estimate the microstrain in (111) and (100) planes, respectively. TEM observations were performed on a JEOL 2010 TEM at an operating voltage of 200 kV. The thin foils for TEM experiments were prepared by means of twin-jet electropolishing with an electrolyte consisting of 25% alcohol, 25% phosphorus acid, and 50% de-ionized water (by volume) that was cooled by liquid nitrogen.

Differential scanning calorimetry (DSC; Perkin-Elmer Pyris 1) was employed to study the thermal characteristics of the nc Cu-Bi sample. The sensitivity of the energy measurement was about 0.01 mJ/g; the temperature of the calorimeter was calibrated by using pure In and Zn standard specimens, with an accuracy of ±0.02 °C. The nc Cu-Bi samples were sealed in aluminum pans and heated in a flowing argon atmosphere at a constant heating rate of 10 °C/min.

Annealing treatments for nc samples were carried out at the temperature range of 160-320 °C for 10 min in a vacuum of 1×10^{-6} Pa. The microstructural evolution of these samples was characterized by XRD and TEM. Vickers microhardnesses of these Cu-Bi samples subjected to various annealing treatments were measured on a MVK-H3 hardness tester with 10 g force load applied for 15 s.

Tensile test was performed on a Tytron 250 Microforce Testing System (MTS) at a strain rate of 6×10^{-3} s^{-1} at room temperature. A contactless MTS LX300 Laser extensometer was used to calibrate and measure the strain. Dog-bone-shaped tensile specimens with a gauge length of 4 mm and a width of 2 mm were prepared by means of electrodischarging from the as-deposited Cu-Bi foils. The final sample thickness after electropolishing is about 30 ± 5 μm.

3. Results

3.1 Structure Characterization

Figure 1 shows the XRD pattern of as-deposited nc Cu-Bi in comparison with that of coarse-grained (CG) polycrystalline pure Cu (annealed at 500 °C for 48 h). It is obvious that in the as-deposited Cu-Bi sample only a fcc Cu phase are identified. The nc Cu-Bi sample exhibits a texture similar to the polycrystalline Cu sample. However, the diffraction lines of the nc Cu-Bi are significantly broadened when compared with those of CG Cu. According to physical broadening profiles, an average grain size of 14 nm and a mean microstrain of about 0.19% are obtained in the as-deposited Cu-Bi.

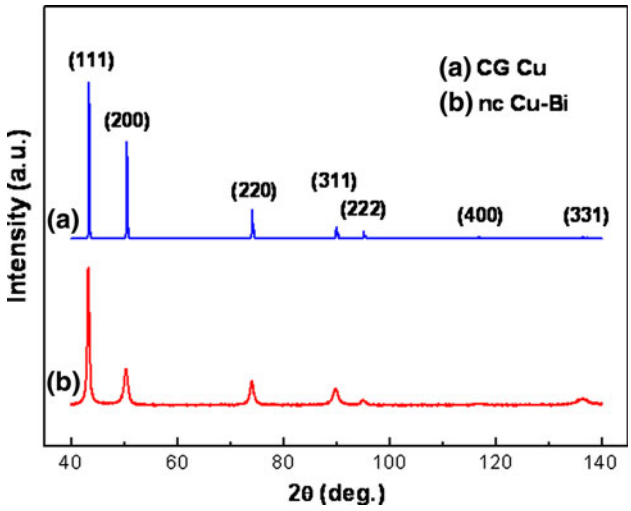

Fig. 1 XRD patterns for as-deposited nc Cu-Bi specimen with mean grain size of 10 nm, compared with that for coarse-grained polycrystalline Cu (annealed at 500 °C for 48 h)

Bright-field and dark-field TEM images of the nc Cu-Bi sample are shown in Fig. 2(a) and (b). Observations suggested that nc grains are mostly equiaxed with random crystallographic orientations as indicated by selected area electron diffraction (SAED) pattern in the inset of Fig. 2(a). Growth twins are present in some nc grains. HRTEM observations in Fig. 2(c) further confirmed the quite tiny grains and no second phases existent in the microstructure, moreover indicated that most nanometer-sized crystallites were separated by high-angle GBs. Synthesis defects such as nanovoids are not observed. A distribution of grain diameters by measuring about 400 grains for as-deposited Cu-Bi sample, shown in Fig. 2(d), yields an average grain size of 10 nm (Fig. 2d), which is roughly comparable to the size determined by XRD. Similar grain size was obtained in inert-gas-consolidated (IGC) Cu-Bi samples by Haubold (Ref 13) and Konrad et al. (Ref 11).

3.2 Thermal behaviour

Figure 3 illustrates the typical DSC curves of as-deposited nc Cu-Bi. When as-deposited nc Cu-Bi was heated at a rate of 10 °C min^{-1} from room temperature to 350 °C, an evident exothermal peak with an onset temperature of 190 °C are detected, of which integrated released enthalpy is about 1.5 J/g. Two possibilities exist for the origin of the exothermal peak, including grain growth and/or strain release (relaxation) in the as-deposited Cu-Bi.

In order to understand microstructural evolution of the nc sample during annealing treatment, TEM analysis has been performed. Figure 4(a), (b), and (c) shows representative bright-field micrographs of this material annealed for 10 min at 160, 200 and 280 °C, respectively. In Figure 4(a), there is a quite slight grain coarsening taking place in the structure, leading to an average grain diameter of 12 nm for the Cu-Bi sample annealed at 160 °C. An annealing treatment at higher temperature (Fig. 4b) results in a relatively obvious grain growth. Several large grains of about 100 nm can be seen in a still small nanocrystalline matrix with a mean grain diameter of around 17 nm. At 280 °C, which corresponds to the region close to the end of the exothermal peak in the DSC curve, the

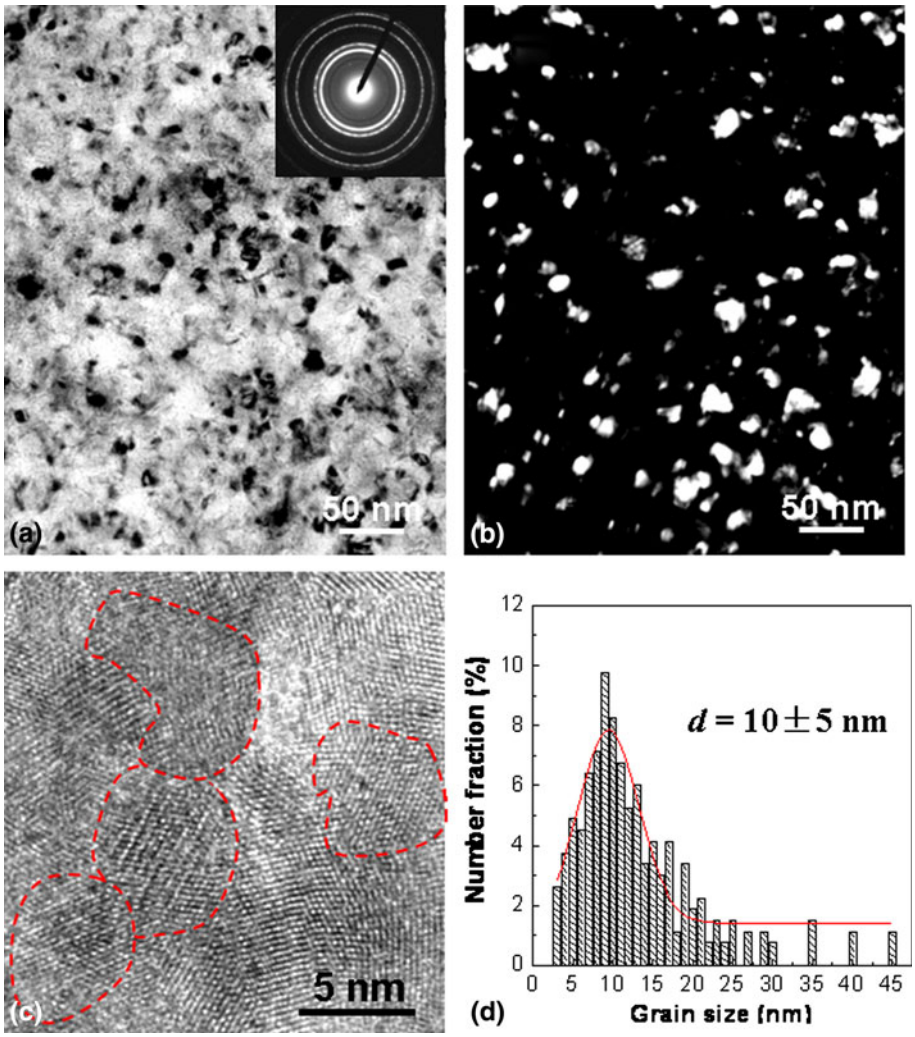

Fig. 2 Bright-field (a) and dark-field (b) TEM images, and HRTEM image (c) of as-deposited nc Cu-Bi specimen. The *inset* of (a) shows the SAED pattern. (d) Statistical grain size distribution determined from TEM observations

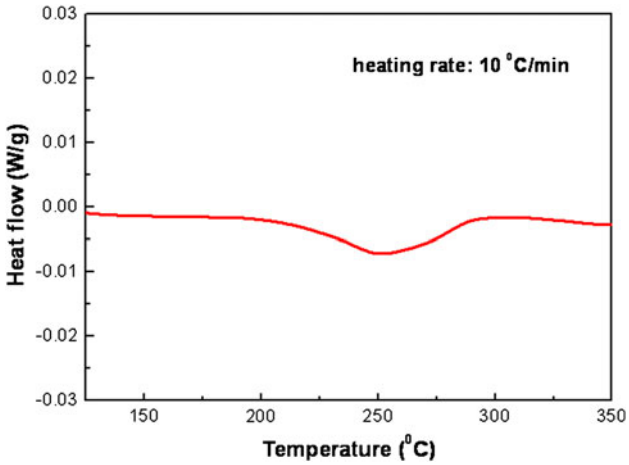

Fig. 3 DSC curve of the as-deposited Cu-Bi sample at a heating rate of 10 °C/min

microstructure contains abundant grown grains. The average grain size increases considerably to 28 nm as determined from TEM dark-field images by carefully measuring 400 crystallites. It was also found that the grains in the annealed samples become more or less better-defined, suggesting the relaxation of grain boundaries during the annealing process.

Figure 5 shows the quantitative XRD analysis results of the electrodeposited nc Cu-Bi sample annealed at different temperatures. In Fig. 5(a), it is interesting to note that in the as-deposited sample, the microstrain in (100) plane (e_{100}, 0.33%) is much higher than the microstrain in (111) plane (e_{111}, 0.13%) and the mean microstrain (e from different crystallographic planes, 0.19%). This is similar with what was detected in electrodeposited nc pure Cu (Ref 14). Almost no change was found in the microstrain when the sample was annealed up to 120 °C. Above 120-140 °C, an obvious drop is observed in e_{100} and e_{111}, while only small decrease is seen in e. The e drops to essentially zero with a wide temperature range of 200-320 °C. Figure 5(b) displays the change of average grain size as a function of annealing temperature for the nc Cu-Bi. One can see that there is no clear change in the average grain size when the annealing temperature was below 140 °C. At temperatures in the range of 140-320 °C, an evident increase in the grain size was observed (from about 14-32 nm). The XRD results on grain diameter variation with annealing temperature are basically consistent with the TEM observations.

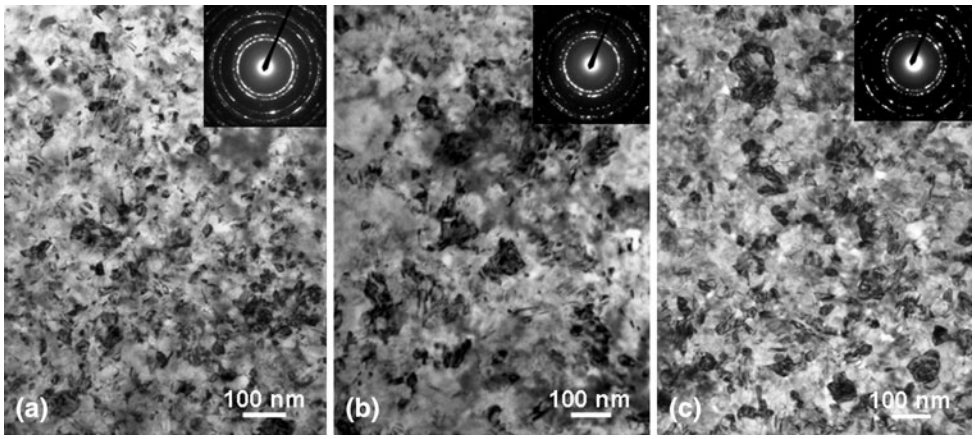

Fig. 4 Plane-view bright-field TEM micrographs of the Cu-Bi samples after annealing at various temperatures for 10 min, (a) 160 °C, (b) 200 °C, (c) 280 °C. The *insets* of (a), (b), and (c) show the corresponding SAED patterns

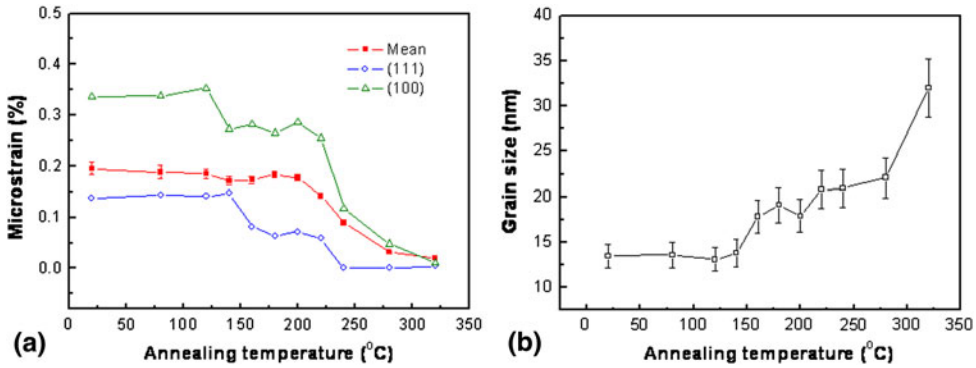

Fig. 5 Variation of microstrain (a) (as indicated) and mean grain size (b) with annealing temperature for the Cu-Bi specimen determined by means of XRD experiments. Annealing duration is 10 min

The dependence of microhardness values on the annealing temperature for the Cu-Bi sample is shown in Fig. 6. The as-deposited nc Cu-Bi has a high hardness of 3.48 GPa, which is higher than that of nc Cu with similar grain diameter prepared by magnetron sputtering (Ref 15). The Cu-Bi sample retains its as-deposited hardness up to the temperature of 160 °C. Anneal softening is first observed when subjected to annealing at 180 °C, which corresponds to the small grain growth and strain relaxation. Annealing at 320 °C results in a ~18% loss in hardness.

3.3 Tensile Properties

Uniaxial tensile true stress-strain curves of the as-deposited nc Cu-Bi and the CG pure Cu are shown in Fig. 7. The nc Cu-Bi sample does not nearly exhibit any plastic strain before failure. It is noted that the nc sample has a substantially higher strength when compared with the CG pure Cu. The ultimate tensile strength reaches as high as 760 MPa, at least one order of magnitude higher than yield strength of the CG Cu sample.

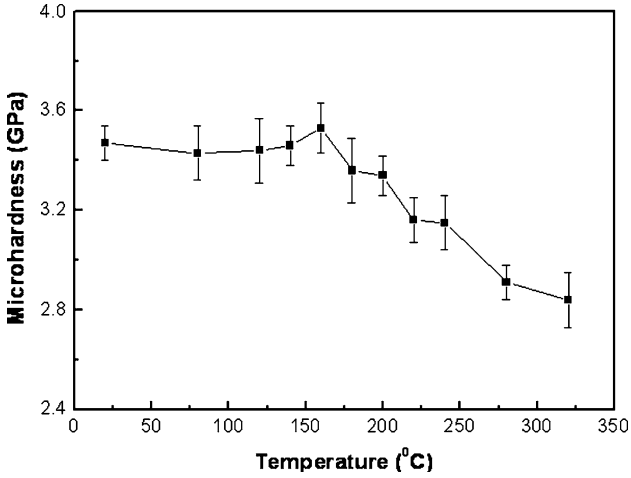

Fig. 6 Variation of microhardness as a function of annealing temperature for the nc Cu-Bi sample. Annealing duration is 10 min. For hardness measurement, 10 g force load is applied for 15 s

4. Discussion

According to the results reported by Chen et al. (Ref 15), dislocation mechanism is still effective in nc Cu with a grain size as small as 10 nm during plastic deformation. Thus, the high strength of the present Cu-Bi sample could dominantly originate from grain refinement effect in nanometer scale, in which lattice dislocation motions are blocked by numerous amounts of GBs. The fact that the tensile strength is much

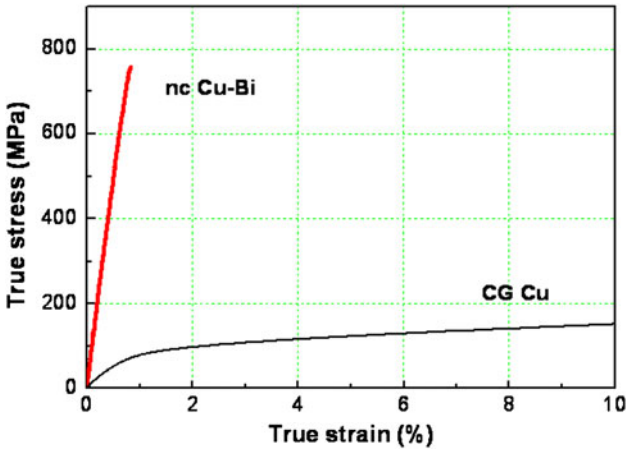

Fig. 7 Tensile true stress-strain curve of the as-deposited nc Cu-Bi sample at room temperature, compared with that of CG pure Cu. The strain rate is 6×10^{-3} s^{-1}

lower than 1/3 hardness, should be related to the preparation flaws that were not detected by TEM. The lack of plastic deformation and tensile necking in the tested nc Cu-Bi sample may be attributed to depressed dislocation activities confined within tiny grains and/or pre-existing flaws.

Based on DSC, TEM, XRD observations, it is obvious that the exothermal peak of DSC curve corresponds to the evident grain growth and major mean microstrain release processes, as indicated in Fig. 4 and 5. At the temperature range of exothermal peak (190-300 °C), the hardness of the Cu-Bi sample experiences a clear drop from 3.48 to 2.85 GPa, which also suggests a softening due to grain coarsening, i.e., GB area decreasing. In fact, there has been a slight growth in grains and a small decrease in microstrain occurring prior to the exothermal signal; however, their thermal effects in the as-deposited nc sample are too weak to be detected by the DSC.

Onset temperature T_{on} of grain growth and heat release ΔH for nc Cu-Bi and nc Cu with various grain sizes reported in the literature (Ref 16, 17) are summarized in Table 1. Also listed in Table 1 are available values of T_{on} and ΔH from the published literature for nc Ni (Ref 18) and Pd (Ref 16). The nc microstructure of as-deposited Cu-Bi specimen starts to become unstable at a temperature of roughly 160 °C. It is worthwhile to note that the value of T_{on} is evidently higher than those reported in the literature. Kumpmann et al. (Ref 16) reported T_{on} = 40 °C in IGC nc Cu with grain size of 40 nm. Klement et al. (Ref 18) obtained T_{on} as low as 84 °C in electrodeposited Ni with the same grain size as the as-deposited Cu-Bi alloy.

The enhanced thermal stability in nc Cu-Bi alloy may be intimately related to low stored energy (reflected by heat release). It is noticed that the heat release in the nc Cu-Bi sample is 1.5 J/g that is only 0.73% of the heat of fusion ΔH_f. This value is much smaller than those for IGC nc Cu with grain size of 40 nm (Ref 16) and high pressure torsion (HPT) nc Cu with grain size of 107 nm (Ref 17). The difference between our measured results and the literature data could be attributed mainly to the difference in GB structures resulting from varying preparation methods and the addition of Bi. Generally, it is the fact that a higher density of GB defects is present in the IGC and HPT samples than the electrodeposited ones. Meanwhile, it is noticed that heat release in the nc Cu-Bi specimen is one order of magnitude less than that in electrodeposited nc Ni with

Table 1 Summary of results on the onset temperature (T_{on}) of grain growth and heat release of nc Cu-Bi sample from present experiments, and comparison with literature data for Cu, Ni, and Pd with different grain sizes

Material	Preparation method	Grain size, nm	T_{on}, °C	Heat release, J/g	References
Cu-Bi	PED	10	160	1.5	This work
Cu	IGC	40	60	5	(Ref 16)
Cu	HPT	107	120	4.1	(Ref 17)
Ni	ED	10	84	18.4	(Ref 18)
Pd	IGC	16	80	16	(Ref 16)

PED, pulse electrodeposition; IGC, inert gas consolidation; HPT, high pressure torsion; ED, electrodeposition

the same grain size, indicating the addition of Bi has a considerable effect on the GB structure and the GB energy in the deposited Cu-Bi. Some studies have revealed that Bi tends to segregate in GBs in IGC nc Cu-Bi (Ref 11, 13). Therefore, for the Cu-Bi alloy, Bi segregation reduces the GB energy and lowers the driving force for grain growth (Ref 7), which contributes to an increase of thermal stability. This is consistent with previous experimental results reported in the literature that grain growth was depressed by the segregation of alloying elements in the GBs of Ni-P, Ni-W, Ni-Mn, Y-Fe, Co-P, and so on (Ref 5, 7-10, 18, 19).

During a grain growth process in a nc material from an initial grain of d_0 to a final size of d (supposing that grain morphology does not change during grain growth), the total grain boundary area in the sample will be deduced by (Ref 20):

$$\Delta S_{gb} = \frac{3W}{2D}\left(\frac{1}{d_0} - \frac{1}{d}\right), \quad \text{(Eq 2)}$$

where W is the sample weight and D is sample density. Here, the sample is assumed to be spherical and the GB thickness is assumed to be 1 nm.

Supposing no shape change of the crystallites takes place and the GB energy γ remains unchanged during the grain growth process, the stored energy concentrated at the GBs, one may get the GB energy from the heat release during the grain growth process by (Ref 20):

$$\gamma = \frac{\Delta H_{gg}}{\Delta S_{gb}} \quad \text{(Eq 3)}$$

TEM results indicate that during the grain growth process, the average grain size of the nc Cu-Bi samples was increased from 10 to about 32 nm. Thus, the GB energy can be estimated to be 0.14 J/m^2 according to Eq 3, quite lower than the value for IGC nc Cu (γ = 0.45 J/m^2) (Ref 16).

5. Conclusions

A Cu-0.42at.%Bi sample with a grain size of 10 nm was prepared by using pulse electrodeposition technique. The as-deposited nc Cu-Bi interestingly exhibits a tensile strength as high as 760 MPa and no plastic deformation takes place prior to failure. Cu-Bi alloy retains its fine-grained microstructure and ultrahigh hardness of ~3.5 GPa up to 160 °C,

indicating a relatively high thermal stability for the Cu-Bi sample. Bi segregating at GBs could facilitate to considerably reduce the grain boundary energy and improve the thermal stability of the as-deposited Cu-Bi alloy.

Acknowledgments

The authors acknowledge the financial support from the National Science Foundation of China (Grant Nos. 50725103, 50621091 and 50890171) and the MOST project of China (Grant No. 2005CB623604).

References

1. M.A. Meyers, A. Mishra, and D.J. Benson, Mechanical Properties of Nanocrystalline Materials, *Prog. Mater. Sci.*, 2006, **51**(4), p 427–556
2. H. Gleiter, Nanocrystalline Materials, *Prog. Mater. Sci.*, 1989, **33**(4), p 223–315
3. A. Gali, H. Bei, and E.P. George, Thermal Stability of Cr-Cr_3Si Eutectic Microstructures, *Acta Mater.*, 2009, **57**(13), p 3823–3829
4. J. Weismmuller, Alloy Effects in Nanostructures, *Nanostruct. Mater.*, 1993, **3**, p 261–272
5. J. Weismmuller, W. Krauss, T. Haubold, R. Birringer, and H. Gleiter, Atomic Structure and Thermal Stability of Nanostructured Y-Fe Alloys, *Nanostruct. Mater.*, 1992, **1**, p 439–447
6. R. Kirchheim, Grain Coarsening Inhibited by Solute Segregation, *Acta Mater.*, 2002, **50**, p 413–419
7. A.J. Detor and C.A. Schuh, Microstructural Evolution During the Heat Treatment of Nanocrystalline Alloy, *J. Mater. Res.*, 2007, **22**(11), p 3233–3248
8. B. Farber, E. Cadel, A. Menand, G. Schmitz, and R. Kirchheim, Phosphorus Segregation in Nanocrystalline Ni-3.6 at.% P Alloy Investigated with the Tomographic Atom Probe (TAP), *Acta Mater.*, 2000, **48**, p 789–796
9. P. Choi, M. da Silva, U. Klement, T. Al-Kassab, and R. Kirchheim, Thermal Stability of Electrodeposited Nanocrystalline Co-1.1%at.P, *Acta Mater.*, 2005, **53**(16), p 4473–4481
10. A.A. Talin, E.A. Marquis, S.H. Goods, J.J. Kelly, and M.K. Miller, Thermal Stability of Mn-Ni Electrodeposits, *Acta Mater.*, 2006, **54**(7), p 1935–1947
11. H. Konrad, T. Haubold, R. Birringer, and H. Gleiter, Nanostructured Cu-Bi Alloys Prepared by Co-Evaporation in a Continuous Gas Flow, *Nanostruct Mater.*, 1996, **7**(6), p 605–610
12. L.-S. Chang, E. Rabkin, B.B. Straumal, B. Baretzky, and W. Gust, Thermodynamic Aspects of the Grain Boundary Segregation in Cu(Bi) Alloys, *Acta Mater.*, 1999, **47**(10), p 4041–4046
13. T. Haubold, Exafs Studies of Bismuth Doped Nanocrystalline Copper, *Acta Metall. Mater.*, 1993, **41**(6), p 1769–1772
14. L. Lu, L.B. Wang, B.Z. Ding, and K. Lu, Comparison of the Thermal Stability Between Electro-Deposited and Cold-Rolled Nanocrystalline Copper Samples, *Mater. Sci. Eng. A*, 2000, **286**(1), p 125–129
15. J. Chen, L. Lu, and K. Lu, Hardness and Strain Rate Sensitivity of Nanocrystalline Cu, *Scripta Mater.*, 2006, **54**(11), p 1913–1918
16. A. Kumpmann, B. Günther, and H.D. Kunze, Thermal Stability of Ultrafine-Grained Metals and Alloys, *Mater. Sci. Eng. A*, 1993, **168**(2), p 165–169
17. R.K. Islamgaliev, F. Chmelik, and R. Kuzel, Thermal Structure Changes in Copper and Nickel Processed By Severe Plastic Deformation, *Mater. Sci. Eng. A*, 1997, **234–236**, p 335–338
18. U. Klement, U. Erb, A.M. El-Sherik, and K.T. Aust, Thermal Stability of Nanocrystalline Ni, *Mater. Sci. Eng. A*, 1995, **203**(1–2), p 177–186
19. G.D. Hibbard, K.T. Aust, and U. Erb, The Effect of Starting Nanostructure on the Thermal Stability of Electrodeposited Nanocrystalline Co, *Acta Mater.*, 2006, **54**(9), p 2501–2510
20. L. Lu, M.L. Sui, and K. Lu, Cold Rolling of Bulk Nanocrystalline Copper, *Acta Mater.*, 2001, **49**(19), p 4127–4134